ELSEVIER

Catalysis Today 41 (1998) 95–109

CATALYSIS TODAY

Supported oxides: Preparation, characterization and catalytic activity of CrO_x/ZrO_2, MoO_x/ZrO_2 and VO_x/ZrO_2

Valerio Indovina

Dipartimento di Chimica, Università degli Studi di Roma "La Sapienza", P.le Aldo Moro 5, 00185 Roma, Italy

Abstract

In the paper, we review the preparation and the characterization of CrO_x/ZrO_2, MoO_x/ZrO_2 and VO_x/ZrO_2. Catalysts were prepared by various methods (equilibrium adsorption, impregnation or mechanical mixing) and characterized by XRD, XPS, ESR and FTIR techniques. In the paper, we also review the catalytic activity of the ZrO_2 supported systems for propene hydrogenation (CrO_x/ZrO_2 and MoO_x/ZrO_2), propane or isobutane dehydrogenation (CrO_x/ZrO_2), abatement of NO with H_2, propane, or propene (CrO_x/ZrO_2), abatement of NO with NH_3 (VO_x/ZrO_2). In selected cases, in order to assess the influence of the support on the catalytic activity, we compare the activity of the MeO_x/ZrO_2 samples with that of the same MeO_x on other supports.

Keywords: Zirconia support; Nitric oxide abatement

1. Introduction

Supported transition metal ions, mainly studied on SiO_2, $A1_2O_3$ and TiO_2, show important catalytic properties. The dispersion, oxidation state, nuclearity and structural features of the supported ion may strongly depend on the support. In turn, all these factors might affect the catalytic activity. It is therefore of interest to study these factors for a given transition metal ion on other supports, in addition to those listed above, and, in particular, on ZrO_2. Zirconia is very stable to thermal treatments, has an amphoteric surface endowed with weakly acid and basic sites, and is able to maintain a high specific surface area up to about 1000 K, if transition metal ions are present.

Supported oxide catalysts are generally prepared by co-precipitation or impregnation. An alternative way to prepare supported catalysts is the equilibrium adsorption method. When an oxide is placed in contact with an aqueous solution, the surface hydroxyl-groups enter into the following equilibria:

$$MeOH_2^+ \leftrightarrow MeOH + H^+ \quad (1)$$

$$MeOH \leftrightarrow MeO^- + H^+ \quad (2)$$

From these equilibria, the solution pH-value at which $[MeO^-]=[MeOH_2{}^+]$, namely the point of zero charge (pzc), can be determined for the various supports. Specifically, $pzc=1/2pK_1+1/2\ pK_2$, where K_1 and K_2 are the equilibrium constants of the reactions (1) and (2), respectively.

For solutions at pH > pzc, the surface of the support is negatively charged and will adsorb cations from the solution, whereas at pH < pzc, the same surface is positively charged and will preferentially adsorb

0920-5861/98/$32.00
PII S0920-5861(98)00041-8

anions. In turn, the solution pH-value also affects the nature of the anions present in solution and, in general, oxoanions of higher nuclearity are formed at lower pH values:

$$\text{Oxoanion(mononuclear)} + n\text{H}^+ \leftrightarrow \text{Polyoxoanion} + \frac{n}{2}\text{H}_2\text{O}$$

As an example, it can be recalled that Wang and Hall [1] have suggested that the nuclearity of the adsorbed Mo species can be controlled by adjusting the pH of the ammonium heptamolybdate solution used for adsorption. For the various supports, the influence of the pH in determining both nuclearity and uptake of the Mo species has been discussed in detail in reviews by Knozinger [2] and Kim et al. [3].

In this paper, we report the preparation and the characterization of CrO_x/ZrO_2, MoO_x/ZrO_2 and VO_x/ZrO_2. In addition to the equilibrium adsorption method, with the aim of assessing the influence of the preparation method, we used other preparation methods (impregnation, mechanical mixing), as specified below. For characterization of samples, we used chemical, XRD, XPS, ESR and FTIR techniques. In agreement with the view expressed by Che [4], we extended the characterization of the catalyst from the very early stages of the preparation (sample as prepared, after thermal treatments at 383 K) to the final stage, when the transition metal ion anchors to the ZrO_2 support. We did this in an attempt to understand the ion–support interaction and how it develops through the various stages of catalyst preparation.

In the paper, we also report the catalytic activity of the ZrO_2 supported systems for propene hydrogenation (CrO_x/ZrO_2), propene hydrogenation and the concomitant metathesis (MoO_x/ZrO_2), propane or isobutane dehydrogenation (CrO_x/ZrO_2), abatement of NO with H_2, propane, or propene (CrO_x/ZrO_2), abatement of NO with NH_3 (VO_x/ZrO_2). In selected cases, in order to assess the influence of the support on the catalytic activity, we compare the activity of the MeO_x/ZrO_2 samples with that of the same MeO_x on other supports.

A list of the papers reporting the preparation, characterization, and catalytic activity of MeO_x/ZrO_2 is given under references, in chronological order [5–24].

2. Preparation of catalysts

The starting material for the preparation of zirconia and of the chromium-, molybdenum- or vanadium-containing specimens was a hydrous zirconium oxide, obtained by precipitation from $ZrOCl_2$ solutions. The precipitation was carried out by bubbling a stream of ammonia-saturated nitrogen for 24 h into a $ZrOCl_2$ solution (final pH=10). The precipitate was washed with water until the Cl^- test gave no visible opalescence, a process which required about 8 h. Some preparations involved a much longer rinsing time, from 48 to 72 h, to get rid of Cl^- as measured in the solid. The precipitate was thereafter dried at 383 K for 24 h. Other zirconium oxides with different textural properties were prepared by subjecting the above material to a final thermal treatment in the range 573–1023 K in air for 5 h, as specified.

The CrO_x/ZrO_2 samples were prepared by bringing into contact the ZrO_2, with a large volume (usually 250 cm^3) of a titrated solution of chromium trioxide. A time of 72 h was seen to be sufficient to reach equilibrium. On the basis of the higher Cr uptake in the acid solution, a pH of 1.0 and a 72 h contact time were adopted as a standard procedure for the preparation. Different Cr contents (wt%) could be obtained by varying the concentration of the contacting solution and/or by varying the temperature T to which the starting hydrous oxide was subjected, and therefore selecting materials with different textures. After impregnation, portions of the specimens were subjected to different heat treatments in air or in oxygen, as specified below. Chromium-containing samples are designated as ZCx(T), where x is the approximate Cr metal content (wt%) and T is the temperature to which the starting zirconium oxide was subjected before chromium uptake, that is, the T value appearing in the symbol $ZrO_2(T)$ of the material used.

The MoO_x/ZrO_2 samples were prepared by: (i) equilibrium adsorption, (ii) impregnation, or (iii) mechanical mixing of ZrO_2 with MoO_3. For equilibrium adsorption, the ZrO_2 support was shaken for 72 h at room temperature (RT) with a solution of ammonium heptamolybdate (AHM, Carlo Erba, RP) at pH 2. A few samples were also prepared at pH 1 or 8. The pH values were fixed by nitric acid or ammonia. For impregnation, the AHM solution was prepared at

pH 2. The catalysts were then dried at 383 K for 24 h and ground into a fine powder. The MoO_x/ZrO_2 catalysts are designated as ZMo*x*(*T*,a), ZMo*x*(*T*,i), or ZMo*x*(*T*,m), where *x* gives the analytical Mo content (wt%), *T* the calcination temperature (K) of the ZrO_2 used as support. The symbols a, i and m specify the preparation method: equilibrium adsorption, impregnation and mechanical mixing, respectively. For samples prepared by equilibrium adsorption, the pH of the AHM solution is also specified as ZMo*x*(*T*,a)pH 1, 2 or 8.

The VO_x/ZrO_2 samples were prepared by three methods: (i) adsorption from a solution of ammonium metavanadate (AV) at pH values of 1–4, adjusted by nitric acid, (ii) dry impregnation with AV solutions and (iii) adsorption from a solution of VO(acetylacetonate)$_2$ in toluene. For adsorption, the ZrO_2 support was shaken for 72 h at RT with the AV solution at pH values of 1–4, fixed by nitric acid. The catalysts were then dried at 383 K for 24 h and ground into a fine powder. The VO_x/ZrO_2 catalysts were designated as ZV*x*pH*y*, where *x* gives the analytical vanadium content (wt%), and *y* the AV solution pH.

The Cr, Mo or V content was determined by atomic absorption (Varian Spectra AA-30) after the sample had been dissolved in a concentrated (40%) HF solution.

The catalysts were studied as prepared (a.p.), or after heating in dry O_2 at 773 K (s.o.), or other thermal treatments in vacuum or in a controlled atmosphere, as specified.

3. Procedures and characterization techniques

For ESR measurements, the activation of samples was performed in an all-glass circulation apparatus equipped with a magnetically driven pump. The catalyst (0.3–0.5 g) was placed in a silica adsorption chamber equipped with a side ESR tube. Samples as prepared were either heated under vacuum at increasing temperature up to 773 K, or submitted to s.o., followed by reduction with CO or H_2 up to 773 K. After evacuation or heating in H_2 or CO, the extent of reduction (*e*/Cr, *e*/Mo or *eN*, number of electrons/total Cr, Mo, or V atoms) was determined from the CO or H_2 consumed at each temperature, or from the O_2 consumed in a subsequent s.o. treatment, measured by means of a pressure transducer (MKS Baratron, sensitivity 10–3 Torr). After evacuation of the a.p. sample at various temperatures, or reduction of the s.o. sample with CO or H_2, the powder was transferred to the ESR tube and the spectrum recorded. ESR measurements were made at RT or at 77 K on a Varian E-9 spectrometer operated at X-band frequencies. The spectrometer was equipped with an on-line computer for data treatment.

For IR measurements, powdered materials were pelleted in self-supporting discs, 25–50 mg cm^{-2} and 0.1–0.2 mm thick, placed in an IR cell allowing thermal treatments in vacuo or in a controlled atmosphere. The IR measurements at RT were carried out on a.p. samples evacuated at increasing temperature from RT to 773 K, and after s.o., followed or not by reduction with CO or H_2 at 773 K. In some cases, after evacuation of a.p. samples or after s.o., samples were exposed to H_2O vapor for various times and evacuated at various temperatures, before carrying out IR measurements at RT. FT-IR spectra were recorded at RT on a Perkin–Elmer 1760-X spectrophotometer equipped with a cryodetector, at a resolution of 2 cm^{-1}.

The X-ray diffraction analysis of a.p. and s.o. samples was carried out by a Philips PW 1710 diffractometer at 45 kV and 20 mA using the Cu K_α radiation. X-ray photoelectron spectra were obtained with a Leybold–Heraeus LHS 10 spectrometer (AI K_α, 1486.6 eV, 12 kV, 30 mA) operating in FAT mode (50 eV pass energy), and interfaced with a Hewlett–Packard 2113B computer.

4. Catalytic experiments

4.1. Propene hydrogenation

After reducing the catalysts to a controlled extent, the catalytic activity for the hydrogenation and metathesis of propene were measured (flow apparatus, GC analysis). The reactant stream (95% H_2, 5% C_3H_6) flowed through the catalyst (20–170 cm^3 min^{-1}) at a pressure of about 100 kPa. The reaction was generally followed for 1 h, with a first analysis after 5 min and then after every 15 min. A marked deactivation with time on stream was observed for hydrogenation, probably due to the formation of carbonaceous species

held strongly on the surface of the catalyst. Therefore, the activity for hydrogenation (expressed as average turnover frequency, N molecules s^{-1} $atom^{-1}$) was calculated from the initial rate at $t=0$.

4.2. Propane or isobutane dehydrogenation

The activity was measured at atmospheric pressure in a flow apparatus consisting of two sections. The first section is an all-glass vacuum line, with a circulation loop of volume 0.15 l equipped with an MKS Baratron pressure transducer (sensitivity 1 N m^{-2}) and a magnetically driven recirculation pump (flow rate $=0.8$ l min^{-1}) for catalyst conditioning and adsorption measurements. The second part is a flow section for catalytic runs. The catalyst (usually 0.5 g) in the form of powder was placed on a fritted disk sealed inside a silica reactor which could be connected to the vacuum line or to the flow section by means of a four-way valve.

In propane dehydrogenation, the analysis of reactants and products was carried out with a gas chromatograph with a column filled with a 60–80 mesh silica gel and employing nitrogen as carrier gas. A temperature program from 343 to 403 K and a FID detector in series to a HWD detector were used. The system allowed the separation of hydrogen, methane, ethane, ethene, propane and propene, in this order. The areas of the gas chromatographic peaks were evaluated by an integrator (Spectra Physics Mod. SP4290). In the isobutane dehydrogenation, C_1–C_4 hydrocarbons were analyzed with a Chrompack Plot column held at 403 K, and a flame ionization detector. Hydrogen was analyzed with a column packed with silica gel operated at RT, and a thermal conductivity detector.

4.3. Abatement of NO with H_2, propane, or propene

The catalysis study was conducted at 523–773 K in a flow apparatus. The reactants and products were analyzed by gas chromatography. The reagent mixture consisted of NO/reducing agent/O_2/He. The reducing agents were H_2, C_3H_8 or C_3H_6. Reagent concentrations were: NO=1000 ppm, H_2=2000 ppm, C_3H_8 and C_3H_6=600–800 ppm, and O_2=1–1.5%.

4.4. Abatement of NO with NH_3

Catalytic experiments were done in an apparatus consisting of a flow measuring and control system, fixed-bed flow microreactor, electrically heated and equipped with a temperature programmer–controller, two on-line IR analyzers, one for NO and the other for NH_3, and an on-line gas chromatograph, equipped with a 2 m length column (Alltech CTR) for the analysis of O_2, N_2 and N_2O. Typical experiments were conducted in the temperature range 473–723 K, feeding a gas mixture containing 700 ppm NO, 700 ppm NH_3 and 3.6% O_2 in helium. The effect of O_2 partial pressure was also tested. The flow rate of the reactant gas was 60 L/h ($W/F=5\times10^{-6}$ g h cm^{-3}). NH_3 was oxidized by feeding a gas mixture containing 700 ppm NH_3 and 3.6% O_2 in helium. Catalytic data were expressed as NO or NH_3 conversion percent, or calculated as apparent kinetic constants (k/NO molecules nm^{-2} s^{-1}), assuming the occurrence of a single reaction ($4NO+4NH_3+O_2=4N_2+6H_2O$), first order with respect to NO and zero order with respect to NH_3.

5. Chromium, molybdenum and vanadium uptake by ZrO_2

Chromium uptake depends on the pH of the solution and on the previous heat treatment of zirconia. The uptake at pH 1 is larger than at pH 8, for any given pretreatment temperature T of $ZrO_2(T)$. The Cr uptake per gram decreases with increasing temperature pretreatment of zirconia, due to the decrease of SA. Since Cr uptake is a surface phenomenon, it is therefore significant to consider the uptake per unit area as represented in Fig. 1, which shows the Cr uptake (Cr atoms nm^{-2}). The dashed line t (slope 1) represents the adsorption of all Cr present in the solution (total adsorption). Curve (a) gives the results for samples based on $ZrO_2(383)$ at pH 1. Curve (b) embraces all other specimens based on $ZrO_2(T)$ at pH 1. Curve (c) refers to samples from $ZrO_2(773)$ at pH 8. The saturation value for $ZrO_2(923)$ is also reported. At pH 1 and at low Cr values, the uptake curve practically follows line t. The amount taken at pH 8 is considerably lower than that taken at pH 1. It is of interest to consider the limiting values of the different curves, which tend to level off. The values

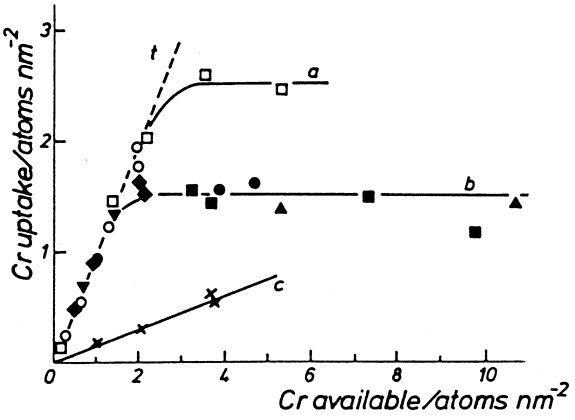

Fig. 1. Chromium uptake. Line t: total adsorption. Curve a: ZrO_2(383)pH1; curve b: Zro_2(573–1023)pH1; curve c: ZrO_2(773)pH8 (adapted from [7]).

are about 2.5 Cr atoms nm^{-2} for samples based on ZrO_2(383) and 1.5–1.9 Cr atoms nm^{-2} for all ZCX(T# 383) specimens.

In the equilibrium adsorption method, the molybdenum uptake on zirconia depended mainly on the pH of the AHM solution used for adsorption and the concentration of the AHM solution itself. At pH 2 and at a moderate AHM concentration, the heptamer ($[Mo_7O_{24}]^{6-}$, HM) is by far the most abundant species in solution. Therefore at this pH, a value substantially lower than the isoelectric point (IEPS) of ZrO_2, HM anions are expected to be adsorbed on the ZrO_2 surface. For samples ZMo*x*(823,a)pH2, the total adsorption increased linearly with the concentration of available Mo, but as the concentration of available Mo increased further, the uptake tended to level off to a value of about 5 Mo atoms nm^{-2}. Samples ZMo5.64(823,a)pH2 and ZMo10.5(823,a)pH2 had a higher Mo content because they were prepared from concentrated AHM solutions (0.01 and 0.05 M), from which octamolybdate anions $(H_2Mo_8O_{28})^{6-}$ tend to polymerize and a precipitate may form. As expected, the surface density was lower on ZMo(823,a)pH8 samples (the uptake levelled off to 1.8 Mo atoms nm^{-2}) than on ZMo(823,a)pH2, due to the pH value being higher than the IEPS of ZrO_2. For samples prepared at pH 1, the AHM concentration and the available Mo were both kept low to avoid precipitation of MoO_3.

For ZV(a)pH2–4 samples, up to 2.5 atoms nm^{-2}, all the available V was adsorbed. As the available V increased further, uptake reached an extended plateau, corresponding to about 3V atoms nm^{-2}. By contrast, for ZV(a)pHl samples, V-uptake progressively increased throughout the region of the available V. The maximum V-uptake was about 2.4 atoms nm^{-2}.

6. Surface species on CrO_x/Zro_2, MoO_x/ZrO_2 and VO_x/ZrO_2

6.1. Cro_x/ZrO_2 samples

Chromium species formed on the zirconia surface after the various treatments along with the identification method are reported in Table 1. Two redox couples, to some extent independent of each other, are identified on the surface of ZC catalysts: Cr(V)/Cr(III) and Cr(VI)/Cr(II). The full reversibility of the two couples and the low nuclearity of the chromium species (as demonstrated by ESR and IR spectroscopies) point to well-dispersed chromium. Strong interaction of chromium with the zirconia matrix prevents its segregation as α-Cr_2O_3. In particular, oxidized ZC catalysts contain isolated Cr(V) ions, surface chromates and especially in more concentrated samples, polynuclear chromium species, polychromates(VI), polychromates(V) and possibly

Table 1
Chromium species on the surface of CrO_x/ZrO_2 catalysts

Treatment	ESR	IR	XPS	Redox cycles	
				n	Species
Oxidized	Cr(V)	Cr(V), Cr(VI)	Cr(VI), Cr(V)	5.5	Cr(VI), Cr(V)
Reduced	Cr(III)-δ	Cr(III), Cr(II)	Cr(III), Cr(VI)	2.5	Cr(III), Cr(II)
Reacted with H_2O	Cr(III)-δ, Cr(III)-β	Cr(III)	Cr(III)	3	Cr(III)

polychromates of mixed valence (VI and V). Since the average oxidation state (n) is n=5.5, Cr(VI) and Cr(V) are present in nearly equal amounts. Upon reduction with CO, isolated Cr(III) species are formed from Cr(V) in the early stages of reduction at lower temperatures. As reduction proceeds, Cr(II) ions are also formed from Cr(VI). In the latter situation, Cr(II)–Cr(III) and Cr(II)–Cr(II) species appear in addition to isolated Cr(II) and Cr(III) species. On fully reduced samples, since n=2.5, Cr(III) and Cr(II) are formed in nearly equal amounts. Finally, the redox potential and the chemical stability of chromium species justify the observed ease of reduction of Cr(V) to Cr(III) along with the ease of the reverse process.

6.2. MoO_x/ZrO_2 *samples*

The analysis of MoO_x/ZrO_2 samples after heating in O_2 at 773 K shows the presence of Mo(VI). A linear correlation is found between the peak area intensity ratios, $I_{(Mo\ 3d)}/I_{(Zr\ 3d)}$, and the surface concentration of Mo, up to about 6 Mo atoms nm^{-2}. The sample ZMo5.64(823), containing 7.7 atoms nm^{-2}, shows evidence of aggregation of molybdenum species (MoO_3 like). Experiments performed on the sample ZMol.36(923) reduced in situ by flowing H_2 at 473–673 K show the presence of Mo(V) in addition to unreduced Mo(VI). The percentage of the Mo(V) species is 30±10% at all reduction temperatures. After reduction at 623 or 673 K, the presence of MO(IV) is also detected.

After s.o. and reduction with H_2 for 10 min at 523 K, an ESR signal detectable at both RT and 77 K, is observed in all ZMo samples. The ESR analysis of spectra of dilute ZMo samples containing 95 Mo allows assigning the signal to a mononuclear Mo(V) species on the surface of ZrO_2. On all samples, the Mo(V) content increases with increasing extent of reduction, up to e/Mo=0.3, and remains almost constant thereafter. The fraction of total Mo detected by ESR as Mo(V) is 0.3 in the most dilute samples and decreases markedly with increasing Mo content.

Samples ZMo were reduced with H_2 at 333–803 K to various extents in a random sequence and reoxidized thereafter with O_2 at 773 K. From these experiments, a linear correlation between the e/Mo values determined from the H_2 consumed and the corresponding values determined from the O_2 consumed is found for all ZMo catalysts. Maximum reduction extents were $(e/\mathrm{Mo})_{H_2} = 3.1$, corresponding to n=2.9.

Upon adsorption of NH_3 at RT on ZMo samples reduced to e/Mo≥0.3 and therefore showing the ESR signal of $Mo_{5c}{}^{V}$ at its maximum intensity, a different Mo(V) species is detected by ESR. The latter species, identified as $Mo_{6c}{}^{V}$ is stable upon evacuation at RT, and is partially transformed in the $Mo_{5c}{}^{V}$ species after evacuation at 473 K. After a subsequent evacuation at 673 K the $Mo_{5c}{}^{V}$ species is irreversibly restored.

6.3. VO_x/ZrO_2 *samples*

For all samples, both a.p. and s.o., irrespective of the preparation method, the experimental XPS intensity ratios, V 2p/Zr 3d, increased proportionally to the V-content up to 3 atoms nm^{-2}. For ZV samples with V-content ≤3 atoms nm^{-2}, this finding shows that vanadium species are uniformly spread on the ZrO_2 surface. On ZV catalysts with a larger V content the intensity ratios V 2p/Zr 3d point to a V surface enrichment.

Because of the intensity of V 2p peaks, which is much lower than that of the nearby O 1s peak, the vanadium oxidation state could be reliably ascertained only for ZV(a) and ZV(i) specimens with a V loading >1% (2.5 atoms nm^{-2}). The binding energy value of the V 2p (3/2) component, obtained by curve fitting of the region O 1s – V 2p, showed V(V) only, in a.p. and s.o. samples, and reduction to V(IV), after heating with CO at 500 K. On the same sample the redox cycle showed e/V=1, corresponding to an average vanadium oxidation state of 4.

In a.p. and s.o. ZV(a) and ZV(i) samples, no ESR signals were detected. In a.p. ZV(acac), a weak ESR signal of vanadyl species was detected (5% of total V), being absent after the s.o. treatment. The spectra of samples reduced with CO at 400–623 K consisted of a signal showing a resolved hyperfine structure (V_h), overlapping a broad (ΔH_{pp}=300 Gauss) and nearly isotropic band (V_b, g_{iso}=1.97). When recorded at 77 K, both V_h and V_b maintained the same shape as at RT, and their intensity as a function of temperature followed the Curie law.

The spectroscopic features of V_h allow the signal to be assigned to mononuclear isolated V(IV) in a square pyramidal configuration (vanadyl species). The

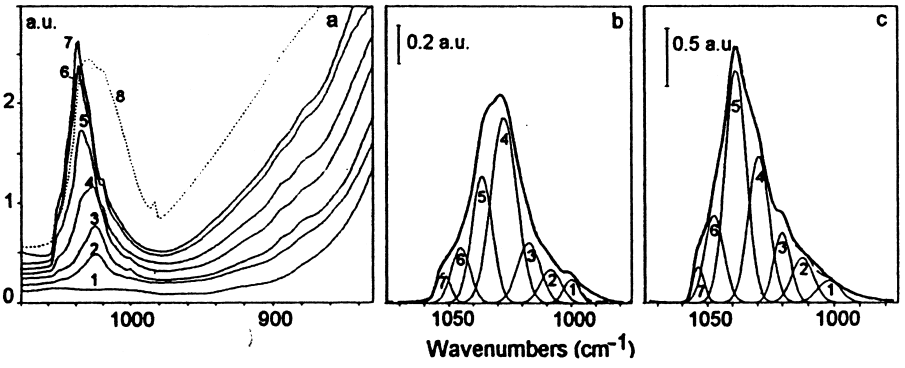

Fig. 2. IR spectra of s.o. samples. Section a: ZrO_2, curve 1; ZV0.18(a)pH4, curve 2; ZV0.30(acac), curve 3; ZV0.58(a)pH4, curve 4; ZV0.83(a)pH4, curve 5; ZV1.05(i) curve 6; ZV1.21(a)pH4, curve 7; ZV4.65(a)pH4, curve 8. Section b: curve fitting of the band at 980–1070 cm^{-1}: 998–1000 cm^{-1}, peak 1; 1007–1008 cm^{-1}, peak 2; 1017–1020 cm^{-1}, peak 3; 1025–1029 cm^{-1}, peak 4; 1034–1038 cm^{-1}, peak 5; 1042–1045 cm^{-1}, peak 6; 1050–1052 cm^{-1}, peak 7. Sample s.o. ZV0.58(a)pH4. Section c: as in Section b. Sample s.o. ZV1.21(a)pH4 (adapted from [24]).

absence of a hyperfine structure and the large value of the line-width of V_b, both features arising from dipolar and exchange interactions among paramagnetic species, suggest its assignment to magnetically interacting V(IV), formed by the reduction of polyoxoanions anchored to the zirconia surface. With increasing V-content, the sequence of ZV sample spectra shows that in the low-loading ZV (up to 0.2 atoms nm^{-2}) isolated mononuclear V(IV) species prevailed, whereas with increasing V-loading interacting V(IV) became prevalent.

Exposure of s.o. samples to NH_3–NO at 623 K caused the formation of a weak V_h signal. A subsequent treatment with NO–NH_3–O_2 mixtures, containing increasing amounts of O_2, caused a progressive decrease in V_h and its disappearance with 1–2% O_2. Exposure to NO–NH_3 of reduced samples (CO at 623 K), therefore containing V_h and V_b, caused a decrease in the ESR detected V(IV) by 65%. After this treatment V_b species were nearly absent. Exposure of reduced samples to NO–NH_3–O_2 caused the complete oxidation of V(IV) species.

In a.p. ZV(a) and ZV(i) samples, broad IR bands arising from hydrated vanadates were detected in the 800–1100 cm^{-1} region. Metavanadate-like species prevailed on ZV samples with V-content <1.5 atoms nm^{-2} and decavanadates (bands at 850–880 and 960–990 cm^{-1}) in the range 1.5–3 atoms nm^{-2}. A.p. ZV(acac) samples showed bands from CH_3 and C=O, suggesting the adsorption of $VO(acac)_2$ as such.

Spectra of s.o. samples differed markedly from those of a.p. samples and were unaffected by a subsequent evacuation up to 673 K (Fig. 2(a)). Spectra consisted of a composite envelope of heavily overlapping bands at 980–1070 cm^{-1}, with two weak bands at 874 and 894 cm^{-1}. Irrespective of the preparation method, the integrated area (cm^{-1}) of the composite band at 980–1070 cm^{-1} was proportional to the V-content up to 3 atoms nm^{-2}. An analysis of spectra by the curve-fitting procedure showed the presence of several V=O modes. The relative intensity of the various peaks contributing to the composite band depended only on the V-content and did not depend on the method used for preparing the catalysts. Samples with V>3 atoms nm^{-2} had IR-spectra features similar to those of pure V_2O_5 (spectrum 8 in Fig. 2(a)).

According to the dependence of the intensity of the various peaks on the V-content, we distinguished vanadates with different nuclearities (roughly three types). The first, corresponding to peak 3 and prevailing in most dilute samples (spectra 2 and 3 Fig. 2(a)), is a low nuclearity species possibly mononuclear (type-I). Type-II vanadates had an increasing concentration in the vanadium range 0.4–0.8 atoms nm^{-2}, peaks 1, 2 and 4 (Fig. 2(b,c)). Type-III vanadates had a markedly increasing concentration in the vanadium range 1.5–3 atoms nm^{-2} and increased little thereafter, peaks 5, 6 and 7 (Fig. 2(b,c)).

At RT, NH_3 adsorbed on Lewis acid sites, Zr(IV) and V(V). Accordingly, the intensity of bands from

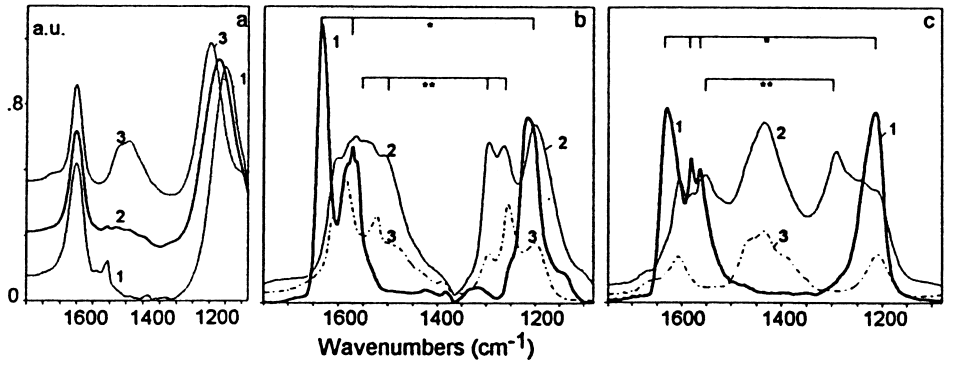

Fig. 3. IR spectra of s.o. samples after various treatments. Section a: after adsorption of NH_3 (1 mbar) at RT: ZrO_2 (curve 1); ZV0.58 (a)pH4 (curve 2); ZV1.21(a)pH4 (curve 3). Section b: ZV0.589a)pH4 sample after adsorption of NO+O_2 at 623 K (curve 1); after subsequent adsorption of NH_3 (1 mbar) at RT (curve 2); and after subsequent heating at 623 K (curve 3). Bands assigned to bridged bidenate nitrates (*) and to chelating nitrates (**). Section c: the same treatments as in Section b on s.o. ZV1.21(a)pH4 (adapted from [24]).

NH_3 decreased little with the V-content, by 15% at most, as expected on account of the similar Lewis acid strengths of Zr(IV) and V(V). The symmetric bending of NH_3 was 1157 cm^{-1} on pure ZrO_2, and shifted to higher frequency on ZV. In particular, on most dilute ZV the frequency band was 1195 cm^{-1} and with increasing V-content it progressively increased up to 1208 cm^{-1} (Fig. 3(a)). NH_4^+ did not form on ZrO_2 and ZV samples with V-content <1.5 atoms nm^{-2}, whereas it did form on more concentrated samples and markedly increased with V-content up to 3 V atoms nm^{-2} (Fig. 3(a)).

At RT, NO adsorption on s.o. ZV samples gave weak bands from N_2O and nitrites. The same species formed on pure ZrO_2. Adsorption of NO+O_2 gave strong bands from bridged bidentate-nitrates (spectra 1 in Fig. 3(b,c)). On both ZV0.58(a)pH4 and ZV1.21(a)pH4, after evacuation at RT, the subsequent addition of NH_3 at RT gave more intense NH_4^+ bands than those on s.o. samples and caused the concomitant transformation of bridged nitrates into chelating nitrates (spectra 2 in Fig. 3(b,c)). NH_4^+ species were much more intense in ZV1.21(a)pH4 than in ZV0.58(a)pH4. A subsequent heating at 623 K caused the disappearance of chelating nitrates in ZV1.21(a)pH4 (spectrum 3 in Fig. 3(c)) and their decrease (to 50%) in ZV0.58(a)pH4 (spectrum 3 in Fig. 3(b)), while surface-OH formed and H_2O and N_2 were detected by analysis of the gas phase.

7. Propene hydrogenation on CrO_x/ZrO_2

The experiments in the circulation apparatus show: (i) pure ZrO_2 is much less active than reduced CrO_x/ZrO_2 catalysts. The activity of the matrix is increased by increasing the heating temperature in vacuum; (ii) the apparent activation energy (E_a) of reduced ZC catalysts is 16±1 kJ $mole^{-1}$ and is independent of the extent of reduction, throughout the whole range from e/Cr=0.8–3.1; (iii) the catalytic activity of the ZC specimens markedly rises with increasing the extent of reduction.

The dependence of activity on the extent of reduction was further investigated at 195 K in the flow apparatus. The results obtained are reported for various ZC catalysts as a plot of $\log N_{Cr}$ as a function of e/Cr or $\tilde{n}$ (Fig. 4). The following main points emerge: (i) A sharp increase in activity (2–3 orders of magnitude) is observed when the extent of reduction is increased from e/Cr=0 to about 2.5 ($\tilde{n}$=5.5–3). Upon further reduction, some decrease in catalytic activity is noticed; (ii) No substantial difference is found when H_2 is used as reducing agent instead of CO. About the same maximum N_{Cr}, and e/Cr values are in fact obtained by reducing the catalysts with either gas; (iii) The catalytic activity is higher when the temperature of evacuation after reduction with CO is increased from 623 to 723 K, especially at lower extents of reduction.

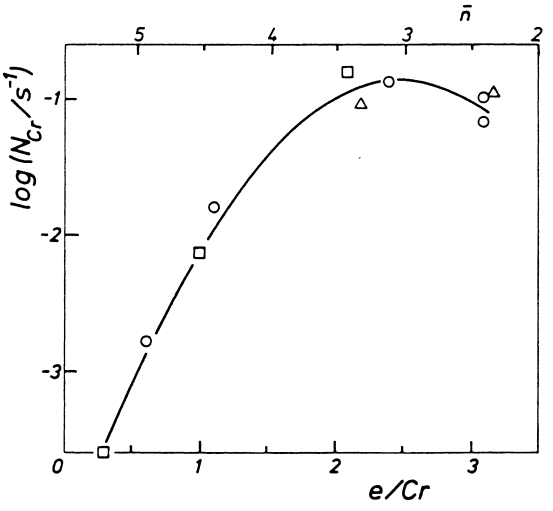

Fig. 4. Turnover frequencies per total chromium atoms (N_{Cr}: C_3H_8 molecules s^{-1} $atom^{-1}$) at 195 K as a function of extent of reduction (*e*/Cr). Catalysts: ZC0.5(923)B*, (○) reduced with CO and evacuated at 723 K (flow); (□) reduced with CO and evacuated at 623 K (circulation); (△) ZC0.5(923)B reduced with H_2 and evacuated at 623 K (circulation) (adapted from [9])

The effect of H_2O vapor was studied on ZC catalysts reduced to the maximum extent by H_2 at 623 K and thereafter reacted with H_2O vapor at various temperatures. The data show that the catalytic activity is unaffected if the sample, after s.o. and reduction with H_2, is reacted with H_2O at either 723 K or at 873 K.

The results allow identifying Cr(III) as the oxidation state involved in the active site, as pointed out by the following considerations: (i) ZC catalysts must be reduced in order to be active, and therefore Cr(VI) and Cr(V) can be ruled out, leaving Cr(III) and Cr(II) as possible candidates; (ii) After reaching the maximum Cr(III) concentration (n=3.0), a constant or a slightly declining activity upon further reduction is observed in the range where more Cr(II) is being formed; (iii) Any role of Cr(II) is also ruled out by the observation that heating the reduced catalyst with water vapor up to 873 K, a process which destroys Cr(II), leaves the catalytic activity practically unchanged. The same argument also excludes any role of Cr(II)–Cr(III) pairs.

Having now focussed on Cr(III) as the active oxidation state, the catalytic results together with the ESR and IR findings show that not all Cr(III) species are equally active. The ESR analysis has shown that two Cr(III) species (different from α-Cr_2O_3) can be distinguished: Cr(III)-δ and Cr(III)-β. The δ species is preferentially formed upon CO reduction of Cr(V), it is mononuclear, and it is not affected by H_2O treatment up to about 873 K. The catalytic activity is high in all states of the catalyst where this species is identified. The β species is formed from the selective oxidation of Cr(II) with water. The ESR analysis shows that it corresponds to a more magnetically concentrated species than δ. The catalytic behavior of the two species appears different.

We conclude that the catalytically active species must be sought among the Cr(III) species belonging to isolated or weakly interacting population. However, not necessarily all of these species are equally active. In fact, the very difference between Cr(III)-δ and Cr(III)-β focusses attention not merely on the oxidation state of Cr, but also on its coordination and on its ligand sphere of interaction. A high coordinative unsaturation, such as is more likely present on isolated or nearly isolated Cr(III) species, is therefore suggested.

8. Hydrogenation and metathesis of propene on MoO_x/ZrO_2

The catalytic activity for the hydrogenation of propene at 298 K, expressed as average turnover frequency, N_h (propane molecules/s/total Mo atoms), is reported in Fig. 5, for some ZMo catalysts as a function of *e*/Mo. If unreduced, all ZMo catalysts are inactive, whereas after reduction to *e*/Mo≥1, a marked increase of activity with increasing extent of reduction is observed.

When comparing samples of different Mo content reduced to about the same extent (*e*/Mo=3), the corresponding N_h values are found to increase strongly (by 2 orders of magnitude) with increasing surface concentration of Mo up to about 5.6 ions nm^{-2}, and are found to decrease thereafter because of segregation of MoO_3-like species (Fig. 5(b)).

The average turnover frequency for the metathesis of propene, N_m (molecules $atom^{-1}$ s^{-1}) as a function of *e*/Mo, is reported in Fig. 6. The catalysts show low activity for metathesis when reduced up to *e*/Mo=1. Above this value a marked increase in activity is

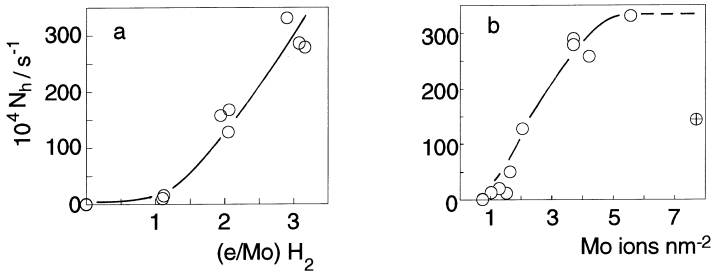

Fig. 5. (a) Turnover frequency at 298 K for propene hydrogenation (N_h: molecules s^{-1} $atom^{-1}$) as a function of the extent of reduction; (b) N_h at 298 K as a function of the Mo surface concentration. Crossed circle: MoO_3 present (adapted from [15]).

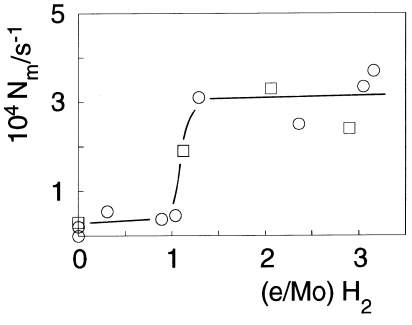

Fig. 6. Turnover frequency at 298 K for propene metathesis (N_m: molecules s^{-1} $atom^{-1}$) as a function of extent of reduction. Samples: (○) ZMo2.09(923)pH=1; (□) ZMo.136(923)pH=2 (adapted from [15]).

observed, whereas metathesis is nearly constant for reduction in the region from *e*/Mo=1–3. The N_m values change but little with increasing Mo surface concentration, up to about 7.7 nm^{-2}. All N_m values are within a factor of 3, if samples are reduced to any extent in the range *e*/Mo=1–3.

Both the interaction between a solute and a surface and the ensuing adsorption process have been discussed by several authors. The role of the surface IEP, and the nature of the solute species have thus received attention. However, their relative importance, as for the case of MoO_x/Al_2O_3, is still being studied. A distinction must be made between the "precursor state", before the treatment of the solid, and after treatment, a process involving dehydration and reduction processes.

After heating the MoO_x/ZrO_2 samples in O_2 at 773 K, Mo(VI)-containing species (molybdates and polymolybdates) are well dispersed on the surface of ZrO_2, provided that the surface concentration of molybdenum does not exceed about 5.6 atoms nm^{-2}. Some aggregation of molybdenum species (MoO_3-like) is observed by XPS in the most concentrated sample (7.7 atoms nm^{-2} sample). A suggestion concerning the nature of surface molybdenum species formed after reduction can be given on the basis of ESR, XPS and $\tilde{n}$ data.

In the early stages of reduction up to 525 K, Mo(V) is the only species detected by either ESR or XPS, in addition to unreduced Mo(VI) detected by XPS. The Mo(V) species is strongly stabilized on the surface of zirconia, as shown by the constancy of its concentration (30%) upon reduction treatments up to 800 K. It should be stressed that almost the same Mo(V) concentration is found when comparing ZMo samples prepared from AHM solutions at different pH. Therefore, for all ZMo samples, irrespective of the pH of AHM solution, a nearly constant molybdates/polymolybdates ratio is inferred from the constant concentration of mononuclear Mo(V) (ESR), which arises from the reduction of mononuclear molybdate species. A buffer effect of the ZrO_2 surface seems to be operating. Specifically, a role of the Brönsted acid–base sites of ZrO_2 can be recognized in the condensation–decondensation of molybdenum anions during heating in O_2 and/or in subsequent reduction with H_2. Thus, whereas the total Mo uptake is mainly controlled by the pH of the AHM solution, the nature of the molybdenum species is to large extent controlled by the nature of the adsorbing oxide.

Upon reducing the catalysts at higher temperature (>525 K), two steep increases of the *e*/Mo parameter are observed when the reduction temperature is increased. The first increase occurs when the temperature is brought from 525 to 600 K, and is attributed to the formation of Mo(IV) by reduction of polymolybdates. The assignment is supported by XPS results,

which show the formation of Mo(IV) in the same temperature region. The second steep increase is attributed to the formation of Mo(0) identified by XPS.

Coming to catalysis, the nature of the active sites in the hydrogenation and metathesis of the ZMo system can be briefly discussed in light of molybdenum species. The marked differences in the behavior of ZMo catalysts toward hydrogenation and metathesis show that distinct sites are operating for the two reactions.

Metathesis is probably carried out on mononuclear Mo(V) species. The statement is supported by (i) the fact that Mo(V) (as detected by ESR) is constant in the same reduction region where the activity for metathesis is also constant and (ii) the facile (structure-insensitive) nature of metathesis on ZMo catalysts. Hydrogenation takes place on more-reduced molybdenum species, possibly Mo(0), as suggested by the progressive and marked increase of N_h. The demanding (structure-sensitive) nature of propene hydrogenation on ZMo catalysts and specifically the marked increase of activity with Mo content suggests the presence of an active site precursor consisting of a polynuclear molybdenum species.

9. Propane and isobutane dehydrogenation on CrO_x/ZrO_2

Fig. 7 illustrates the dependence of the dehydrogenation reaction rate on chromium surface concentration for various temperatures. Here, for a series of samples, the specific initial dehydrogenation rate, $r_{(s)}$ (molecules s^{-1} nm^{-2}), is plotted vs. the Cr surface concentration of the sample. In Fig. 7(b), the lines represent the best fittings (least square method) of the $r_{(s)}$ values of ZC catalysts (open symbols). It is noteworthy that: (i) the reaction rate increases with Cr chromium content, (ii) a linear increase satisfactorily represents the experimental data, (iii) at any temperature, the extrapolation to abscissa=0 shows a positive intercept, which represents a contribution not related to the Cr component. This underlines the need to examine the activity of the support. Moreover, since zirconia activity depends on the extent of surface hydration, it was essential to measure the dehydrogenation rate of zirconia in the same experimental conditions as those of the ZC samples. The results for the support are shown in Fig. 7 b as solid symbols at abscissa=0. It can be seen that the intercepts of the lines drawn for ZC catalysts satisfactorily match the experimentally measured activity of the support.

10. The abatement of NO with H_2, propene or propane on CrO_x/ZrO_2

In the presence of oxygen, neither α-Cr_2O_3 nor ZC, CrO_x/SiO_2 (SC) and $CrO_x/A1_2O_3$ (AC) samples showed activity for NO reduction with either propene or propane. Pure ZrO_2 was active for the selective catalytic reduction of NO (SCR), but with each hydrocarbon it produced a considerable amount of CO in

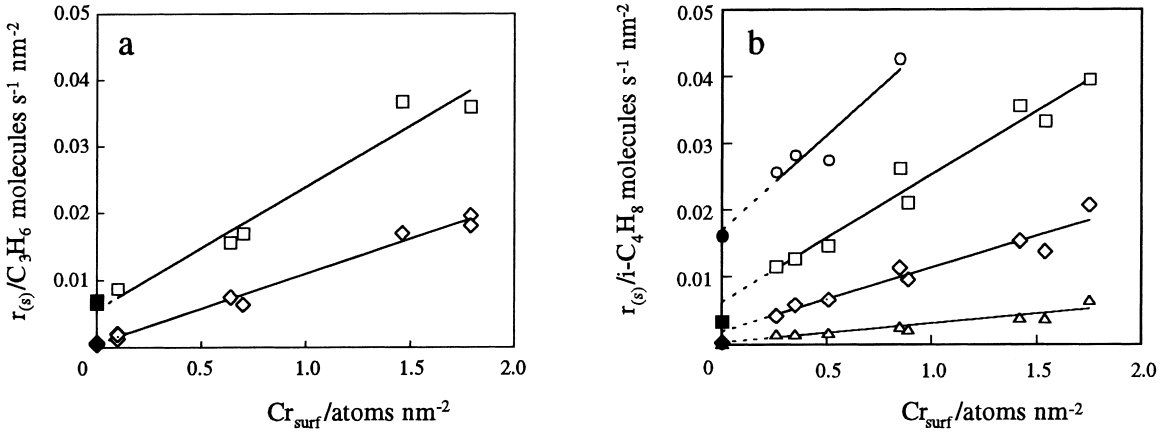

Fig. 7. Specific dehydrogenation rate of (a) propane and (b) isobutane vs. chromium surface concentration for ZC catalysts. △, ▲ 673 K; ♢, ◆ 723 K; □, ■ 773 K; ○, ● 823 K (adapted from [17]).

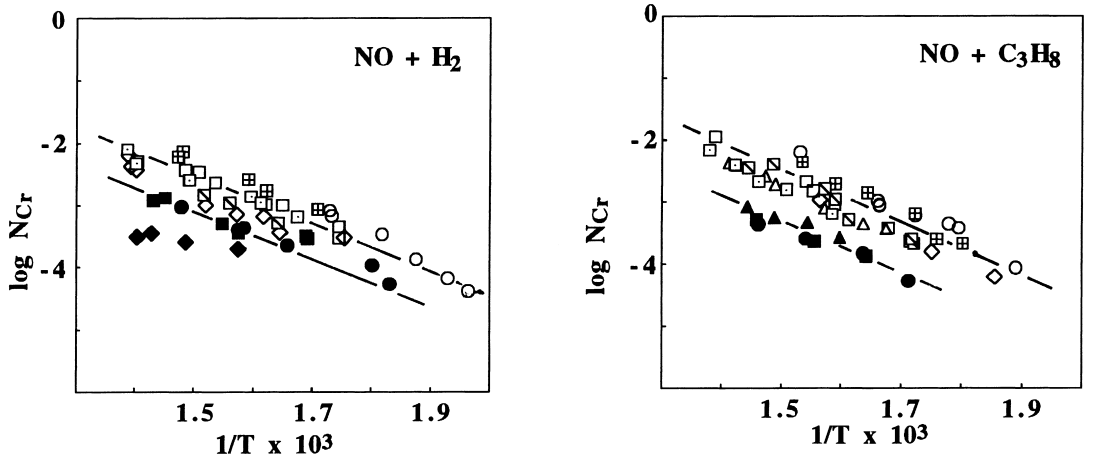

Fig. 8. Turnover frequency (N_{Cr}: NO molecules s^{-1} Cr-atom^{-1} for the reduction of NO by H_2 (left) or C_3H_8 (right) on α-chromia (○), CrO_x/ZrO_2 (ZC0.04, Δ, ZC0.14, ◇, ZC0.29, □), CrO_x/SiO_2 (SC0.08, ◇ SC0.17, □, SC0.44, □), CrO_x/Al_2O_3 (AC0.16, ▲, AC0.62 ■, AC1.6, ●) (adapted from [23]).

addition to CO_2. On the addition of chromium, the SCR activity of ZrO_2 decreased with chromium content.

In the absence of oxygen, α-Cr_2O_3, ZC and SC samples, after a short initial decay, showed stable catalytic activity and selectivity to N_2 ($SN=N_2/N_2+N_2O$) for both the NO+H_2 and NO+C_3H_8 (or C_3H_6) reactions. AC samples exhibited lower stability. On replacing propane with propene, the activity level of the ZC samples rose slightly, whereas the activity of the SC and AC samples remained unchanged.

The Arrhenius plot for NO+H_2 and NO+C_3H_8 (Fig. 8), showing constant N_{Cr} values at any chromium content and at a given T within each system (ZC, SC and AC), suggests that active sites consist of mononuclear chromium species. Because N_{Cr} would otherwise have increased with chromium concentration, the constancy of N_{Cr} also suggests that special active site configurations, such as pairs of Cr–O–Cr arrangements, are unnecessary. The results also show that the catalytic activity depends little on the reducing agent and support (compare ZC with SC, Fig. 8).

Surprisingly, the N_{Cr} values on α-Cr_2O_3 were close to those measured on ZC and SC. The AC catalysts, particularly the aged ones, were somewhat less active than the other chromium containing catalysts.

The selectivity to N_2 on α-Cr_2O_3, ZC and AC samples depended little on the Cr content and reducing agent. The selectivity increased with the reaction temperature, approaching 100% at $T \geq 643$ K. SC samples generally showed lower N_2 selectivity.

NO adsorption at RT caused the formation of chromium mononitrosyls and dinitrosyls on the surface of all catalysts investigated here. On ZC, AC and α-Cr_2O_3, nitrites and N_2O were also formed. Nitrates formed only on ZC samples. The absence of nitrites and nitrates on SC rules out a role of both nitrites and nitrates in the abatement of NO, otherwise the various chromium-supported samples would have shown markedly diverse catalytic activity.

One important reason suggesting that dinitrosyls, rather than mononitrosyls, and particularly the Cr(III) dinitrosyls, participate in the abatement of NO is the fact that the products, N_2 and N_2O, require N-atom pairing.

A fact which supports Cr(III) dinitrosyls is their suitable stability. In particular, $Cr^{III}(NO)_2$ species are still present on ZC, SC, AC and α-Cr_2O_3 surface even after the samples have been heated in vacuo at 423 K. Moreover, after their disappearance by heating in vacuo at a higher temperature, $Cr^{III}(NO)_2$ species are reversibly restored by a new NO admission.

A fact suggesting the participation of Cr(III) rather than Cr(II) is the poor stability of Cr(II) in the presence of H_2O, which is produced in all reactions examined here. In a more direct way, we found that

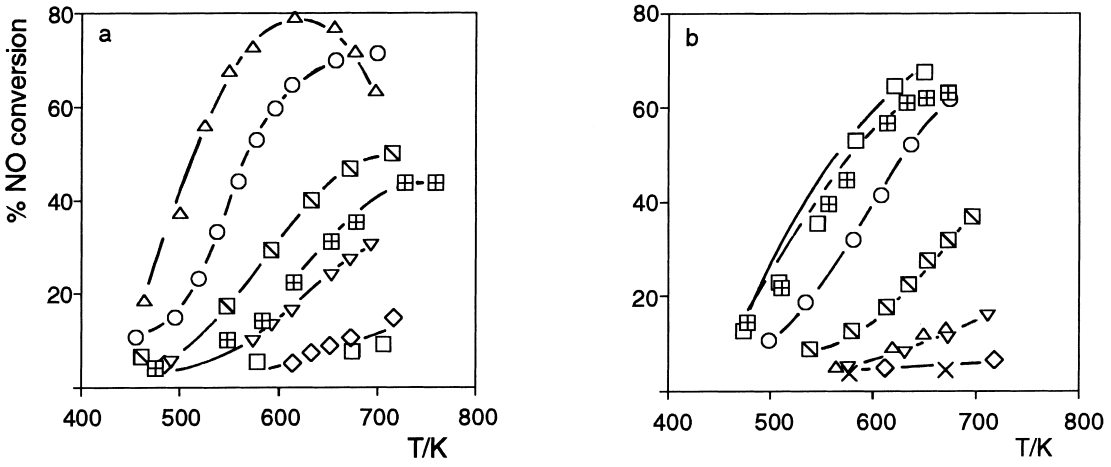

Fig. 9. NO conversion (%) vs. temperature. Section a: (□) ZV0.18(a)pH4; (◇) ZV0.34(a)pH4; (□) ZV0.58(a)pH1; (□) ZV0.60(a)pH4; (□) ZV0.83(a)pH4; (○) ZV1.17(a)pH4; (△) ZV4.79(a)pH4. Section b: (◇)ZV0.17(i); (△)ZV0.32(i); (□)ZV0.64(i); (□) ZV1.05(i); (△)ZV0.30 (acac); (○)ZV0.96(acac); (□) ZV1.36 (acac); (x) ZrO_2 (adapted from [24]).

the addition of H_2O in excess to the reactant mixture did not affect the catalytic activity of SC samples. The behavior of Cr(III) dinitrosyls in the presence of $NO+H_2$ appears to confirm their participation in the abatement reaction. At the temperature at which catalysis occurs, the infrared spectra show that Cr(III) dinitrosyls progressively disappear while N_2O and H_2O are produced.

11. The selective catalytic reduction of NO with ammonia on VO_x/ZrO_2

On all catalysts, the activity for SCR was stable as a function of the time on stream and the ratio NO/NH_3 remained very close to unity.

In samples ZV(a) (Fig. 9(a)), ZV(i) and ZV(acac) (Fig. 9(b)), NO conversion increased with V-loading

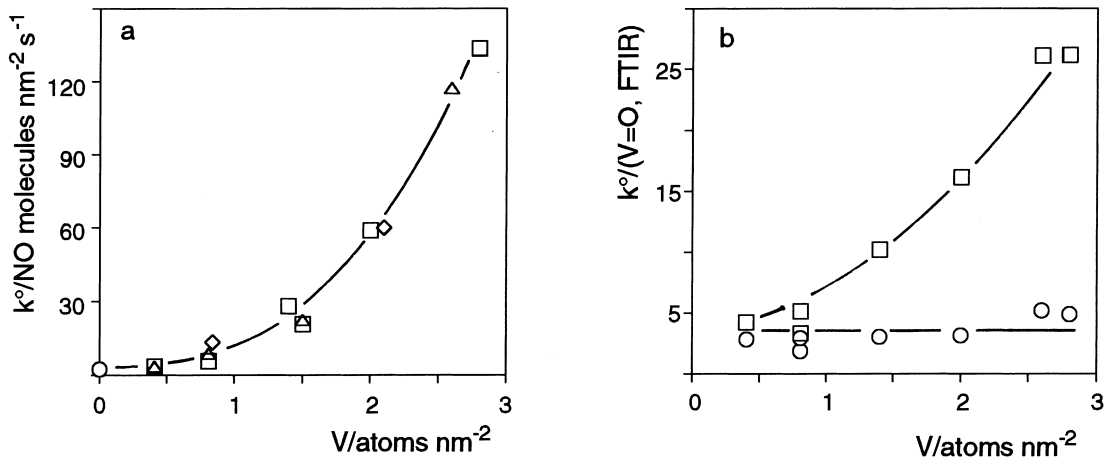

Fig. 10. The dependence of catalytic activity on the V-content (a) and its correlation with type-III polyoxovanadates (b). Section a: 10^{-3} k° vs. V-content on ZrO_2 (○), ZV(a) (□), ZV(i) (△), and ZV(acac) (◇). Section b: 10^{-2} k° divided by the total integrated area (cm^{-1}) of bands in the region 980–1070 cm^{-1} (□), and 10^{-3} k° divided by the sum of components 5, 6 and 7 (○) areas (cm^{-1}) (adapted from [24]).

at all temperatures. In the whole temperature range, the selectivity to N_2 was very high. Small amounts of N_2O ($\leq$3%) were detected only above 573 K. Pure zirconia showed some SCR activity at $T \geq 573$ K, comparable with that of ZV0.18(a)pH4. The best performance was obtained with the catalyst ZV1.17(a)pH4, containing 2.8 V atoms nm^{-2}, namely a V-content close to that of the adsorption plateau in ZV(a) samples (3 atoms nm^{-2}).

On the sample ZV4.79(a)pH4 (12.6 V atoms nm^{-2}) containing segregated V_2O_5, NO conversion reached a maximum at 623 K and decreased thereafter. Higher reaction temperatures resulted in the formation of very large amount of N_2O ($\geq$10%) arising from the oxidation of NH_3; NH_3 conversion still monotonically increased with the temperature.

In all ZV catalysts, the apparent activation energy (E_a kJ mol^{-1}) was nearly independent on the V-content (42$\pm$4 kJ mol^{-1}). Therefore, the dependence of catalytic activity on the V-content can be conveniently inspected through k° values, the pre-exponential factor of the Arrhenius equation. The finding that k° values, irrespective of the method used for preparing the catalyst, stay on the same curve, shows that the SCR activity is mainly controlled by the vanadium content (Fig. 10(a)). The marked and non-linear increase of k° with the V-content clarifies that the concentration of the active vanadium is not proportional to the V-loading, i.e., only specific configurations are active. To identify the active vanadium configuration, we divided k° values by the intensity of (i) the composite band at 980–1070 cm^{-1}, (ii) peak corresponding to type-I vanadates, (iii) peaks of type-II polyvanadates, and (iv) peaks of type-III polyvanadates. Normalized k° values monotonically and markedly increase by a factor 8–11, but normalized k° values for type-III polyoxovanadates remain about constant, well within a factor of 2 (Fig. 10(b)).

12. Conclusions

While the pH of solutions used in the equilibrium adsorption determines the Mo and uptake, the pH neither affects the nature of surface molybdates or vanadates, nor the relative concentration of the various nuclearity species. A comparison of samples of similar concentration shows that the surface distribution species, namely the monomers/polymers ratio, is the same on samples prepared by equilibrium adsorption or impregnation. All these findings suggest that buffer effect of the ZrO_2 surface operates toward condensation–decondensation of anions during the heating of samples in O_2 at 773 K. Thus, rather than being controlled by the pH of the solution, the nuclearity of molybdenum and vanadium is controlled mostly by the acid–base properties of the support sites.

The dependence of catalytic activity on the transition metal content and extent of reduction has allowed us to put forward reasonable hypotheses on the nature of the active sites (oxidation state and nuclearity) for various reactions.

References

[1] L. Wang, W.K. Hall, J. Catal. 77 (1982) 232.
[2] H. Knozinger, in: M.J. Phillips, M. Teman, (Eds.), Proceedings Ninth International Congress on Catalysis, vol. 5, Chem. Inst. Canada, Ottawa, 1988, p. 20.
[3] D.S. Kim, K. Segawa, T. Soeya, I.E. Wachs, J. Catal. 136 (1991) 744.
[4] M. Che, in: L. Guczi, F. Solymosi, P. Tetenyi (Eds.), Proceedings of the Tenth International Congress on Catalysis, vol. A, Budapest, 1993, p. 31.
[5] A. Cimino, D. Cordischi, S. De Rossi, G. Ferraris, D. Gazzoli, V. Indovina, G. Minelli, M. Occhiuzzi, M. Valigi, Characterization of chromia/zirconia catalysts and their activity in hydrogen–deuterium equilibration and propene hydrogenation, in: M.J. Phillips, M. Teman (Eds.), Proceedings of the Ninth International Congress on Catalysis, vol. 3, Calgary, 1988, p. 1465.
[6] A. Cimino, D. Cordischi, S. Febbraro, D. Gazzoli, V. Indovina, M. Occhiuzzi, M. Valigi, F. Boccuzzi, A. Chiorino, G. Ghiotti, The nature of surface chromium species on CrO_x/ZrO_2 catalysts, J. Mol. Catal. 55 (1989) 23.
[7] A. Cimino, D. Cordischi, S. De Rossi, G. Ferraris, D. Gazzoli, V. Indovina, G. Minelli, M. Occhiuzzi, M. Valigi, Studies on chromia/zirconia catalysts. I. Preparation and characterization, J. Catal. 127 (1991) 744.
[8] A. Cimino, D. Cordischi, S. De Rossi, G. Ferraris, D. Gazzoli, V. Indovina, M. Occhiuzzi, M. Valigi, Studies on chromia/zirconia catalysts. II. ESR of chromium species, J. Catal. 127 (1991) 761.
[9] A. Cimino, D. Cordischi, S. De Rossi, G. Ferraris, D. Gazzoli, V. Indovina, M. Valigi, Studies on chromia/zirconia catalysts. III. Propene hydrogenation, J. Catal. 127 (1991) 777.
[10] V. Indovina, D. Cordischi, S. De Rossi, G. Ferraris, G. Ghiotti, A. Chiorino, The adsorption of O_2 and NO on CrO_x/ZrO_2 catalysts as investigated by IR and ESR spectroscopies, J. Mol. Catal. 68 (1991) 53.

[11] D. Cordischi, V. Indovina, M. Occhiuzzi, Exchange coupled Cr^{V} and Mo^{V} ions on the surface of CrO_x/ZrO_2 and MoO_x/ZrO_2, as investigated by ESR spectroscopy, J. Chem. Soc. Faraday Trans. 87 (1991) 3443.

[12] S. De Rossi, G. Ferraris, S. Fremiotti, A. Cimino, V. Indovina, The dehydrogention of propane on CrO_x/ZrO_2, Appl. Catal. 81 (1992) 113.

[13] D. Cordischi, V. Indovina, M. Occhiuzzi, The dispersion of Cr^{V} and Mo^{V} on the surface of various oxides, as investigated by ESR spectroscopy, Appl. Surf. Sci. 55 (1992) 233.

[14] V. Indovina, A. Cimino, S. De Rossi, G. Ferraris, G. Ghiotti, A. Chiorino, The nature of the active site for propene hydrogenation on CrO_x/ZrO_2 catalysts, J. Mol. Catal. 75 (1992) 305.

[15] V. Indovina, A. Cimino, D. Cordischi, S. Della Bella, S. De Rossi, G. Ferraris, D. Gazzoli, M. Occhiuzzi, M. Valigi, The catalytic activity of MoO_x/ZrO_2 in the hydrogenation and metathesis of propene, in: L. Guczi, F. Solymosi, P. Tetenyi (Eds.), Proceedings of the Tenth International Congress on Catalysis, vol. A, Budapest, 1993, pp. 875–887.

[16] M. Valigi, A. Cimino, D. Cordischi, S. De Rossi, C. Ferrari, G. Ferraris, D. Gazzoli, V. Indovina, M. Occhiuzzi, Molybdenum (VI) interaction with zirconia surface and its influence on the crystallization and sintering, Solid State Ionics 63–65 (1993) 136–142.

[17] S. De Rossi, G. Ferraris, S. Fremiotti, V. Indovina, A. Cimino, lsobutane dehydrogenation on chromia/zirconia catalysts, Appl. Catal. 106 (1993) 125–141.

[18] D. Cordischi, M.C. Campa, V. Indovina, M. Occhiuzzi, The structure of Cr^{V} species on the surface of various oxides: reactivity with NH_3 and H_2O, as investigated by ESR spectroscopy, J. Chem. Soc. Faraday Trans. 90 (1994) 207–212.

[19] D. Gazzoli, F. Prinetto, M.C. Campa, A. Cimino, G. Ghiotti, V. Indovina, M. Valigi, Characterisation of MoO_x/ZrO_2 system by XPS and IR spectroscopies, Surf. Interface Anal. 22 (1994) 398–402.

[20] S. De Rossi, G. Ferraris, S. Fremiotti, E. Garrone, G. Ghiotti, M.C. Campa, V. Indovina, Propane dehydrogenation on chromia/silica and chromia/alumina catalysts, J. Catal. 148 (1994) 36–46.

[21] M.C. Campa, V. Indovina, S. De Rossi, G. Ferraris, G. Ghiotti, A. Chiorino, F. Prinetto, The catalytic activity of CrO_x/ZrO_2 for the $NO+H_2$ reaction, Appl. Catal. B 4 (1994) 257–273.

[22] F. Prinetto, G. Cerrato, G. Ghiotti, A. Chiorino, M.C. Campa, D. Gazzoli, V. Indovina, The formation of the Mo^{VI} surface phase on MoO_xZrO_2 catalysts, J. Phys. Chem. 99 (1995) 5556–5567.

[23] M.C. Campa, G. Ferraris, S. De Rossi, G. Ghiotti, F. Prinetto, V. Indovina, The abatement of NO on CrO_x/SiO_2, $CrO_x/A1_2O_3$ and Cr/ZrO_2, in: G. Centi, S. Perathoner, C. Cristiani, P. Forzatti (Eds.), Proceedings of the World Congress Environmental Catalysis, Pisa, 1995, p. 291–294.

[24] V. Indovina, M. Occhiuzzi, P. Ciambelli, D. Sannino, G. Ghiotti, F. Prinetto, The activity of VO_x/ZrO_2 for the selective catalytic reduction of NO with NH_3, Studies in surface science and catalysis, vol. 101, 1996, Elsevier, p. 691.